

Effects of metallicity on mode switching in Cepheids

Yu. A. Fadeyev*

*Institute of Astronomy, Russian Academy of Sciences, Pyatnitskaya ul. 48, Moscow, 119017
Russia*

Received April 12, 2020; revised May 13, 2020; accepted May 13, 2020

Abstract — The mode switching in Cepheids is studied using the methods of the nonlinear theory of stellar pulsation, depending on the main sequence mass M_0 and the abundance of elements heavier than helium Z . The grid of evolutionary and hydrodynamic models of core–helium burning Cepheids is represented by 30 evolutionary sequences of stars with initial masses $5.7M_{\odot} \leq M_0 \leq 7.2M_{\odot}$ and $Z = 0.014, 0.018, 0.022$. For considered values of Z the periods of the fundamental mode and the first overtone at the oscillation mode switching are shown to depend on the mean density of the stellar matter. The upper limit of the period of the first overtone decreases with increasing Z from ≈ 6.9 day for $Z = 0.014$ to ≈ 4.1 day for $Z = 0.022$. The theoretical period–radius relation is independent of Z and agrees well (within 2.5%) with recent measurements of Cepheid radii based on the Baade–Wesselink method. The fundamental parameters of the short–period Cepheid CG Cas were derived with application of observational estimates of the period and the rate of period change. This star is shown to be the first–overtone pulsator.

Keywords: *stellar evolution; stellar pulsation; stars: variable and peculiar; Cepheids*

INTRODUCTION

At present the General Catalogue of Variable Stars (Samus’ et al. 2017) contains the data on nearly 640 Cepheids (i.e., δ Cep pulsating variables designated as DCEP and DCEPS). Periods of light variations of these stars range from ≈ 2 day to several dozen days. All Cepheids with periods $\Pi > 7$ day are the fundamental mode pulsators, whereas variability of many Cepheids with $\Pi < 7$ day is due to instability of the first overtone. Unfortunately, the particular threshold periods of the fundamental mode and the first overtone corresponding to the mode switching in Cepheids do not exist as in the case of RR Lyr type variables. This is the cause of significant uncertainties arising in distinguishing the pulsation mode of Cepheids with periods $5 \text{ day} \lesssim \Pi \lesssim 7 \text{ day}$. The lack of the observational criterion for mode distinguishing leads to uncertainties in the period–radius and period–luminosity relations because the fundamental mode and the first overtone pulsators follow different relations (Ferne 1968; Böhm–Vitense

*E-mail: fadeyev@inasan.ru

1988, 1994; Sachkov 2002). One of the possible solutions based on the Fourier decomposition of the Cepheid light curve was proposed by Antonello and Poretti (1986) but it can only be applied in the case of high precision photometric measurements.

The periods of the fundamental mode Π_0^* and the first overtone Π_1^* corresponding to oscillation mode switching are described with good accuracy as a function of mean density $\bar{\rho} = M/(\frac{4}{3}\pi R^3)$, where M and R are the mass and the radius of the Cepheid (Fadeyev 2020). This conclusion is based on results of consistent stellar evolution and nonlinear stellar pulsation calculations for Cepheid models with main sequence masses $5.1M_\odot \leq M_0 \leq 6.1M_\odot$ and the abundance of elements heavier than helium $Z = 0.02$. However recent estimates of the galactic abundance gradient obtained from spectroscopic observations of Cepheids are $d[\text{Fe}/\text{H}]/dR_G \approx -0.06 \text{ kpc}^{-1}$ and imply significant variation of the metal abundance Z as a function of galactocentric distance R_G of the star (Andrievsky et al. 2002; Lemasle et al. 2008; Luck and Lambert 2011; Luck et al. 2011.; Genovali et al. 2014; Minniti et al. 2020). Therefore, the dependencies $\Pi_0^*(\bar{\rho})$ and $\Pi_1^*(\bar{\rho})$ for other values of Z remain uncertain.

The goal of the present study is to determine the dependencies $\Pi_0^*(\bar{\rho})$ and $\Pi_1^*(\bar{\rho})$ for Cepheids with metal abundancies $Z = 0.014, 0.018$ and 0.022 . The initial conditions necessary for solution of the equations of radiation hydrodynamics and time-dependent convection describing nonlinear stellar pulsations are obtained from the grid of evolutionary sequences computed from the zero age main sequence to the stage of helium exhaustion in the stellar core. Evolutionary sequences were computed for stars with initial masses $5.7M_\odot \leq M_0 \leq 7.2M_\odot$ with the mass step $\Delta M_0 = 0.1M_\odot$. The initial abundance of helium is assumed to be $Y = 0.28$.

EVOLUTIONARY SEQUENCES OF CEPHEIDS

As in the previous work of the author (Fadeyev 2020) the initial conditions for equations of radiation hydrodynamics describing stellar pulsations were determined from selected stellar models of evolutionary sequences computed with the program MESA version 12778 (Paxton et al. 2019). Convective mixing was treated according to the standard theory (Böhm–Vitense 1958) with mixing length to pressure scale height ratio $\alpha_{\text{MLT}} = \Lambda/H_P = 1.6$. Extended convective mixing (overshooting) at convective boundaries was calculated using the prescription of Herwig (2000) with parameters $f = 0.016$ and $f_0 = 0.004$. Effects of semiconvection were taken into account according to Langer et al. (1985) with efficiency parameter $\alpha_{\text{sc}} = 0.1$ in the expression for the diffusion coefficient D_{sc} .

To inhibit irregular growth of the convective core accompanied by appearance of spurious loops in the HR-diagram the evolutionary calculations of the core helium burning stage were carried out with option 'conv_premix_avoid_increase'. The sufficiently small amplitude of central helium abundance jumps was reached owing to significant increase of the mass zone

number of the evolutionary model ($N \sim 4 \times 10^4$) together with reduction of the time step up to $\Delta t_{\text{ev}} = 10^3$ yr.

The rate equations for nucleosynthesis were solved for the reaction network consisting of 26 isotopes from hydrogen ^1H to magnesium ^{24}Mg with 81 reactions. Calculation of reaction rates was carried out using the JINA Reaclib data (Cyburt et al. 2010). Mass loss due to the stellar wind was computed by the Reimers (1975) formula with parameter $\eta_{\text{R}} = 0.3$.

The role of metallicity in evolution of Cepheids is illustrated in Fig. 1 where the evolutionary tracks in vicinity of the second crossing and the third crossing of the instability strip are shown in the HR diagram for stars with initial mass $M_0 = 6.2M_{\odot}$ and metal abundances $Z = 0.014, 0.018, 0.022$. Parts of the evolutionary track with pulsations in the fundamental mode and the first overtone are shown by dashed and dotted lines, respectively.

Differences between evolutionary tracks shown in Fig. 1 are mainly due to the fact that the opacity and the gas density in the envelope of the pulsating star increase with increasing Z . The radial dependencies of the opacity κ and the gas density ρ are shown in Fig. 2 for three hydrostatically equilibrium Cepheid models with different values of Z . These models correspond to the mode switching during the second crossing of the instability strip and are marked in Fig. 1 by open circles.

In Cepheid models considered in the present study the radius of the node of the first overtone is $r_{\text{n}} \approx 0.80R$, where R is the radius of the upper boundary of the hydrostatically equilibrium model. The necessary condition for pulsations in the first overtone is that the helium ionizing zone driving pulsation instability should locate in layers with radial distance $r > r_{\text{n}}$. This condition is not fulfilled for models of the evolutionary sequence $Z = 0.022, M_0 = 6.2M_{\odot}$ during the third crossing of the instability strip so that the Cepheid evolves between the blue and red edges of the instability strip as the fundamental mode pulsator (see Fig. 1).

RESULTS OF STELLAR PULSATION CALCULATIONS

In this study we computed 30 evolutionary sequences for stars with initial metal abundances $Z = 0.014, 0.018, 0.022$ and initial masses $5.7M_{\odot} \leq M_0 \leq 7.1M_{\odot}$. Selected models of evolutionary sequences corresponding to stages of the second crossing and the third crossing of the instability strip were used as initial conditions for solution of the equations of radiation hydrodynamics and turbulent convection. The equations of the problem are discussed in the earlier paper of the author (Fadeyev 2013). Determination of the instability strip edges as well as calculation of the pulsation period of the hydrodynamic model and the star age at the mode switching is described by Fadeyev (2019). The dependence $\Pi(t_{\text{ev}})$ was approximated by the algebraic polynomial of the 3-rd order for the evolutionary time interval with continuous change of the period.

The main goal of this work is to determine the periods of the fundamental mode Π_0^* and the first overtone Π_1^* at the pulsation mode switching for evolutionary sequences with specified values of Z and M_0 . Results of calculations are shown in Fig. 3, where periods Π_0^* and Π_1^* are plotted as a function of the mean stellar density $\bar{\rho}$. As is seen, these dependencies are independent of Z within the margin of error and are given by relations

$$\log \Pi_0^* = -1.475 - 0.539 \log \bar{\rho}, \quad (1)$$

$$\log \Pi_1^* = -1.600 - 0.528 \log \bar{\rho}. \quad (2)$$

The plots in Fig. 3 illustrate the fact that periods of the fundamental mode and the first overtone at the mode switching increase with increasing mass and increasing radius of the Cepheid (i.e. with decreasing $\bar{\rho}$) irrespective of Z . Decrease of the stellar mean density is accompanied by extension of the helium ionizing zone so that pulsations in the first overtone become impossible once the lower boundary of the ionizing zone reaches the node of the first overtone. As seen in Fig. 3, the interval of existence of oscillations in the first overtone (i.e. with period $\Pi_1 < \Pi_1^*$) reduces with increasing Z .

For the sake of clarity, properties of the models at the upper limit of existence of the first overtone oscillations are listed in Table 1. First three columns of Table 1 give the metal abundance Z , initial stellar mass M_0 and the number of the instability strip crossing i . The fourth and the fifth columns give the stellar mass M and the mean density $\bar{\rho}$ at the mode switching. Last two columns give the pulsation periods Π_0^* and Π_1^* . It should be noted that during the second crossing of the instability strip ($i = 2$) the radial pulsations switch from the fundamental mode to first overtone, whereas during the third crossing ($i = 3$) pulsations switch from the first overtone to the fundamental mode.

PERIOD–RADIUS RELATION

Measurements of Cepheid radii using the Baade–Wesselink method (Baade, 1926; Wesselink, 1946) provide the basis for the period–radius relation of galactic Cepheids which is applied for calibration of the period–luminosity relation (Kervella et al. 2004; Turner 2010; Molinaro et al. 2011; Lazovik and Rastorguev 2020). The period–radius relation is derived for fundamental mode pulsators and the Cepheids pulsating in the first overtone are included by multiplication of the period by the constant factor. For example, Lazovik and Rastorguev (2020) used the factor 1.41 to this end.

On the whole, in the present work we computed 326 hydrodynamic models of Cepheids, where 193 models are the fundamental mode pulsators and 133 models are the first overtone pulsators. The pulsation period of the hydrodynamic model was calculated using the discrete

Fourier transform of the kinetic energy of pulsation motions (Fadeyev 2013). Together with period of the principal mode we evaluated also the period of the secondary mode. In the fundamental mode pulsator the role of the secondary mode is played by the first overtone, whereas in the case of the first overtone pulsator the role of the secondary mode belongs to the fundamental mode. The period ratio of the fundamental mode and the first overtone was found to be $\Pi_0/\Pi_1 \approx 1.50$ and independent of the locus with respect to the mode switching.

The period–radius relations obtained from the present evolutionary and hydrodynamic calculations are shown in Fig. 4. As in Fig. 3, the plots in Fig. 4 do not show any dependence on Z , so that the periods and radii locate near the straight lines f_0 and h_1 which are given by

$$\log R/R_\odot = 1.203 + 0.631 \log \Pi_0 \quad (3)$$

and

$$\log R/R_\odot = 1.281 + 0.685 \log \Pi_1, \quad (4)$$

where the pulsation period is expressed in days.

For hydrodynamic models considered in the present study the lower limit of the fundamental mode period is $\Pi_0 = 5.59$ day, whereas the upper limit of the first overtone is $\Pi_1 = 6.57$ day. In the range of these two values the fundamental mode to first overtone period ratio evaluated from (3) and (4) varies within $1.49 \leq \Pi_0/\Pi_1 \leq 1.56$. As seen in Fig. 4, the scatter of period ratios around $\Pi_0/\Pi_1 = 1.50$ is due to variation of radii near the regression line.

In recent years different realizations of the Baade–Wesselink technique have been developed in order to improve the accuracy of Cepheid radius measurements, so that at present there is a number of empirical period–radius relations. These methods were briefly reviewed by Lazovik and Rastorguev (2020). In the present work the theoretical period–radius relation (3) was compared with empirical relations derived by Sachkov et al. (1998), Turner and Burke (2002), Kervella et al. (2004), Storm et al. (2004), Groenewegen (2007), Molinaro et al. (2011), Gallenne et al. (2017), Lazovik and Rastorguev (2020). The best agreement of the theoretical relation (3) with empirical period–radius relation was found for

$$\log R/R_\odot = 1.17 + 0.66 \log \Pi_0 \quad (5)$$

derived by Lazovik and Rastorguev (2020). In Fig. 4 relation (5) is shown by the dotted line. For fundamental mode pulsators with period $\Pi = 5.6$ day the difference between (3) and (5) does not exceed $\approx 2.6\%$, whereas for periods $\Pi \approx 15$ day the difference between the theory and observations becomes as small as $\approx 0.2\%$, so that the theoretical and empirical plots become almost the same.

FUNDAMENTAL PARAMETERS OF THE CEPHEID CG CAS

The short-period Cepheid CG Cas ($\Pi = 4.3656$ day) is observed in the corona of the young open cluster Berkeley 58 and is of great interest for calibration of the period–luminosity relation. The $O - C$ diagram of CG Cas spans somewhat more than a hundred years and is fitted by the parabolic dependence indicating the secular period growth with rate $\dot{\Pi} = 0.170$ s/yr (Turner et al. 2008). Thus, there is an opportunity to evaluate the fundamental parameters of this star on the basis of consistent stellar evolution and nonlinear stellar pulsation calculations. However, the earlier attempt to determine the fundamental parameters of CG Cas for the evolutionary sequences with metal abundance $Z = 0.02$ failed because the upper limit of the first overtone period was found to be shorter than the period of CG Cas (Fadeyev 2020).

As seen in Fig. 3 and 4, for evolutionary sequences with metal abundances $0.014 \leq Z \leq 0.022$ the radial pulsations with period $\Pi = 4.3656$ day in the fundamental mode should be excluded since the lower limit of the fundamental mode period is $\Pi = 5.59$ day. Thus, to reconcile the theory with observations we have to admit that CG Cas is the first overtone pulsator. The plots of the period change rate as a function of the first overtone period during the third crossing of the instability strip are shown in Fig. 5 for several evolutionary sequences with $Z = 0.014$ and $Z = 0.018$. Each plot displays the evolution of Π and $\dot{\Pi}$ between the blue edge of the instability strip and the mode switching from the first overtone to the fundamental mode.

As seen in Fig. 5, the evolutionary sequences $Z = 0.014$, $M_0 = 5.7M_\odot$ and $Z = 0.018$, $M_0 = 6.1M_\odot$ are the nearest to the observational estimates of Π and $\dot{\Pi}$. Substitution of $\Pi = 4.3656$ day into dependencies $\Pi(t_{ev})$ of these evolutionary sequences yields the star age t_{ev} and, therefore, its mass, radius and luminosity. The fundamental parameters of the Cepheid CG Cas are listed in Table 2, where in the last column we give the metallicity index of the evolutionary sequence evaluated for the solar metal abundance $Z_\odot = 0.0134$ (Asplund et al. 2009). The metallicity index of CG Cas is $[\text{Fe}/\text{H}] = 0.09$ (Genovali et al. 2014) therefore the model of the evolutionary sequence $Z = 0.018$, $M_0 = 6.1M_\odot$ seems to be the most preferable.

Bearing in mind the results presented above we have to note that in the works devoted to calibration of the period–luminosity relation on the basis of Gaia trigonometric parallaxes (Ripepi et al. 2019; Breuval et al. 2020) the Cepheid CG Cas is improperly considered as a fundamental mode pulsator.

CONCLUSIONS

Dependence of the stellar opacity on Z significantly affects the gas density in the stellar envelope and location of the pulsation driving zone with respect to the node of the first overtone.

Increase of the mass and the radius of the Cepheid is accompanied by decreasing mean density and increasing width of the helium ionizing zone responsible for excitation of oscillations. Pulsations in the first overtone become impossible when the inner boundary of the helium ionizing zone reaches the node of the first overtone during pulsation motions. Increase of periods Π_0^* and Π_1^* corresponding to the mode switching is due to decrease of the gas density in the envelope of the pulsating star. Existence of the upper limit Π_1^* implies that the necessary condition for oscillations in the first overtone is not fulfilled for $\Pi_1 > \Pi_1^*$.

The lower period limit of radial pulsations in the fundamental mode is $\Pi_0^* = 5.59$ day for models of the evolutionary sequence $Z = 0.022$, $M_0 = 5.9M_\odot$, whereas the upper period limit of oscillations in the first overtone is $\Pi_1^* = 6.87$ day for $Z = 0.014$, $M_0 = 7.1$. In other words, for metal abundances $0.014 \leq Z \leq 0.022$ Cepheids can oscillate in the fundamental mode with periods $\Pi > 5.6$ day, whereas oscillations in the first overtone are possible with periods $\Pi < 6.9$ day. However the index of metallicity of the most of Cepheids with accurate measurements of the iron abundance decrease from $[\text{Fe}/\text{H}] = 0.27$ at the galactocentric distance $R_G = 5$ kpc to $[\text{Fe}/\text{H}] = 0.27$ at $R_G = 17$ kpc (Genovali et al. 2014). Adopting the solar galactocentric distance to be $R_{G\odot} = 7.94$ kpc (Groenewegen et al. 2008) and the solar metal abundance $Z_\odot = 0.0134$ (Asplund et al. 2009) we find that in the present work we considered the models with metallicity indices $0.012 \leq [\text{Fe}/\text{H}] \leq 0.215$. Therefore, the Cepheid models computed in the present study are mostly confined to stars located between the Sun and the center of Galaxy, albeit this region can be somewhat wider due to natural dispersion of metallicity in Cepheids. Extension of the Cepheid grid to lower Z will allow us to consider the stars with galactocentric distances greater than the solar galactocentric distance and may lead to somewhat larger values of Π_1^* . Enlargement of Π_1^* due to decrease of Z can be evaluated from additional evolutionary and hydrodynamic computations.

REFERENCES

1. S.M. Andrievsky, V.V. Kovtyukh, R.E. Luck, J.R.D. Lépine, D. Bersier, W.J. Maciel, B. Barbuy, V.G. Klochkova, V.E. Panchuk, and R.U. Karpishek, *Astron. Astrophys.* **381**, 32 (2002).
2. E. Antonello and E. Poretti, *Astron. Astrophys.* **169**, 149 (1986).
3. M. Asplund, N. Grevesse, A.J. Sauval, and P. Scott, *Annual Rev. Astron. Astrophys.* **47**, 481 (2009).
4. W. Baade, *Astronomische Nachrichten* **228**, 359 (1926).
5. E. Böhm–Vitense, *Zeitschrift für Astrophys.* **46**, 108 (1958).
6. E. Böhm–Vitense, *Astrophys. J.* **324**, L27 (1988).
7. E. Böhm–Vitense, *Astron. J.* **107**, 673 (1994).
8. L. Breuval, P. Kervella, R.I. Anderson, A.G. Riess, F. Arenou, B. Trahin, A. Mérand, A. Gallenne, W. Gieren, J. Storm, G. Bono, G. Pietrzyński, N. Nardetto, B. Javanmardi, V. Hocdé, *Astron. Astrophys.* **643**, A115 (2020).
9. R.H. Cyburt, A.M. Amthor, R. Ferguson, Z. Meisel, K. Smith, S. Warren, A. Heger, R.D. Hoffman, T. Rauscher, A. Sakharuk, H. Schatz, F.K. Thielemann, and M. Wiescher, *Astrophys. J. Suppl. Ser.* **189**, 240 (2010).
10. Yu.A. Fadeyev, *Astron. Lett.* **39**, 306 (2013).
11. Yu.A. Fadeyev, *Astron. Lett.* **45**, 353 (2019).
12. Yu.A. Fadeyev, *Astron. Lett.* **46**, 324 (2020).
13. J.D. Fernie, *Astrophys. J.* **151**, 197 (1968).
14. A. Gallenne, P. Kervella, A. Mérand, G. Pietrzyński, W. Gieren, N. Nardetto, and B. Trahin, *Astron. Astrophys.* **608**, A18 (2017).
15. K. Genovali, B. Lemasle, G. Bono, M. Romaniello, M. Fabrizio, I. Ferraro, G. Iannicola, C.D. Laney, M. Nonino, M. Bergemann, R. Buonanno, P. François, L. Inno, R.–P. Kudritzki, N. Matsunaga, S. Pedicelli, F. Primas, and F. Thévenin, *Astron. Astrophys.* **566**, A37 (2014).
16. M.A.T. Groenewegen, *Astron. Astrophys.* **474**, 975 (2007).

17. M.A.T. Groenewegen, A. Udalski, and G. Bono, *Astron. Astrophys.* **481**, 441 (2008).
18. F. Herwig, *Astron. Astrophys.* **360**, 952 (2000).
19. P. Kervella, D. Bersier, D. Mourard, N. Nardetto, and V. Coudé du Foresto, *Astron. Astrophys.* **423**, 327 (2004).
20. N. Langer, M.F. El Eid, and K.J. Fricke, *Astron. Astrophys.* **145**, 179 (1985).
21. Ya.A. Lazovik and A.S. Rastorguev, *Astron. J.* **160**, 136 (2020).
22. B. Lemasle, P. François, A. Piersimoni, S. Pedicelli, G. Bono, C.D. Laney, F. Primas, and M. Romaniello, *Astron. Astrophys.* **490**, 613 (2008).
23. R.E. Luck and D.L. Lambert, *Astron. J.* **142**, 136 (2011).
24. R.E. Luck, S.M. Andrievsky, V.V. Kovtyukh, W. Gieren, and D. Graczyk, *Astron. J.* **142**, 51 (2011).
25. J.H. Minniti, L. Sbordone, A. Rojas–Arriagada, M. Zoccali, R. Contreras Ramos, D. Minniti, M. Marconi, M.; V.F. Braga, M. Catelan, S. Duffau, W. Gieren, W.; and A.A.R. Valcarce, *Astron. Astrophys.* **640**, A92 (2020).
26. R. Molinaro, V. Ripepi, M. Marconi, G. Bono, J. Lub, S. Pedicelli, and J.W. Pel, *Mon. Not. R. Astron. Soc.* **413**, 942 (2011).
27. B. Paxton, R. Smolec, J. Schwab, A. Gaulty, L. Bildsten, M. Cantiello, A. Dotter, R. Farmer, J.A. Goldberg, A.S. Jermyn, S.M. Kanbur, P. Marchant, A. Thoul, R.H.D. Townsend, W.M. Wolf, M. Zhang, and F.X. Timmes, *Astrophys. J. Suppl. Ser.* **243**, 10 (2019).
28. D. Reimers, *Problems in stellar atmospheres and envelopes* (Ed. B. Baschek, W.H. Kegel, G. Traving, New York: Springer-Verlag, 1975), p. 229.
29. V. Ripepi, R. Molinaro, I. Musella, M. Marconi, S. Leccia, and L. Eyer, *Astron. Astrophys.* **625**, A14 (2019).
30. M.E. Sachkov, *Astron. Lett.* **28**, 589 (2002).
31. M.E. Sachkov, A.S. Rastorguev, N.N. Samus', and N.A. Gorynya, *Astron. Lett.* **24**, 377 (1998).
32. N.N. Samus', E.V. Kazarovets, O.V. Durlevich, N.N. Kireeva, and E.N. Pastukhova, *Astron. Rep.* **61**, 80 (2017).

33. J. Storm, B.W. Carney, W.P. Gieren, P. Fouqué, D.W. Latham, and A.M. Fry, *Astron. Astrophys.* **415**, 531 (2004).
34. D.G. Turner, *Astrophys. Space Sci.* **326**, 219 (2010).
35. D.G. Turner and J.F. Burke, *Astron. J.* **124**, 2931 (2002).
36. D.G. Turner, D. Forbes, D. English, P.J.T. Leonard, J.N. Scrimger, A.W. Wehlau, R.L. Phelps, L.N. Berdnikov, and E.N. Pastukhova, *MNRAS* **388**, 444 (2008).
37. A.J. Wesselink, *Bulletin of the Astronomical Institutes of the Netherlands* **10**, 91 (1946).

Table 1. Upper limits of the periods of the fundamental mode Π_0^* and the first overtone Π_1^* at the mode switching

Z	M_0/M_\odot	i	M/M_\odot	$\lg \bar{\rho}$	Π_0^* , day	Π_1^* , day
0.014	7.1	2	7.055	-4.620	10.312	6.868
	6.5	3	6.451	-4.578	9.844	6.536
0.018	6.5	2	6.469	-4.388	7.741	5.170
	6.2	3	6.162	-4.360	7.467	4.997
0.022	6.2	2	6.175	-4.200	6.142	4.118
	6.1	3	6.074	-4.194	6.063	4.111

Table 2. Fundamental parameters of the Cepheid CG Cas

Z	M_0/M_\odot	$t_{\text{ev}}, 10^6\text{yr}$	M/M_\odot	L/L_\odot	R/R_\odot	T_{eff}, K	[Fe/H]
0.014	5.7	76.217	5.664	3075	52.16	5955	0.019
0.018	6.1	67.256	6.065	3429	53.39	6049	0.128

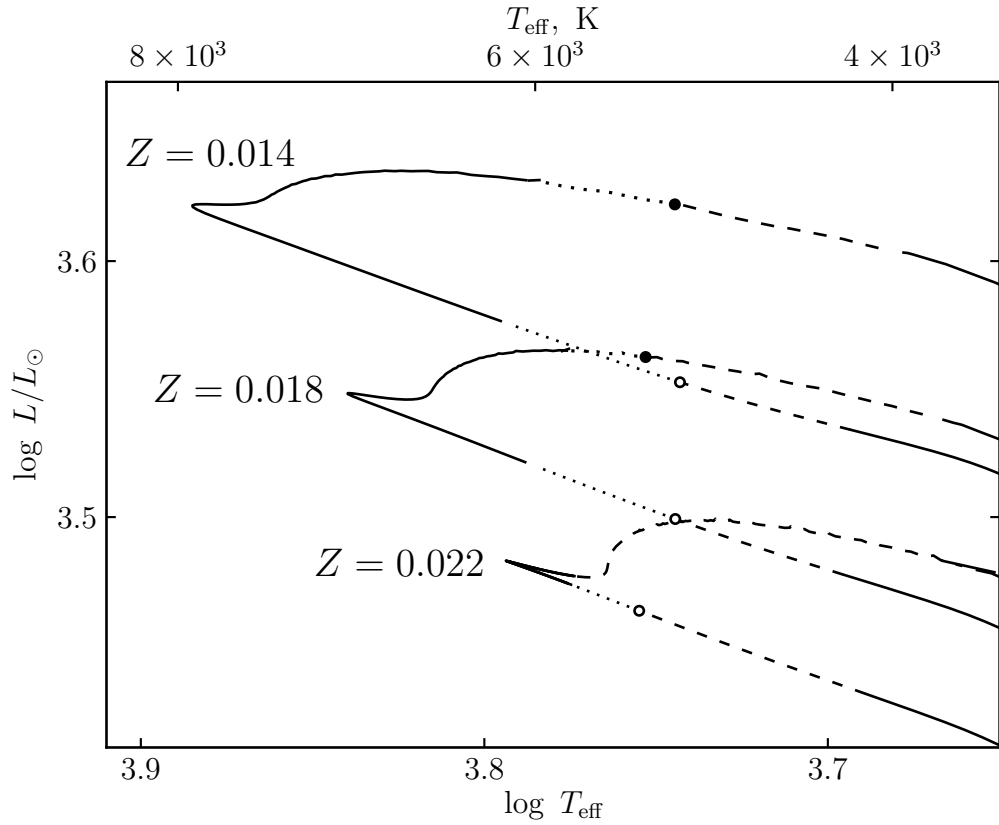


Fig. 1. Evolutionary tracks of stars with initial mass $M_0 = 6.2M_\odot$ for metal abundances $Z = 0.014$, 0.018 and 0.022 in vicinity of the Cepheid instability strip. Parts of the evolutionary tracks where the star does not pulsate are shown by solid lines. The dashed and the dotted lines indicate the stages when the Cepheid pulsates in the fundamental mode and in the first overtone, respectively. Open and filled circles correspond to the mode switching during the second and the third crossings of the instability strip.

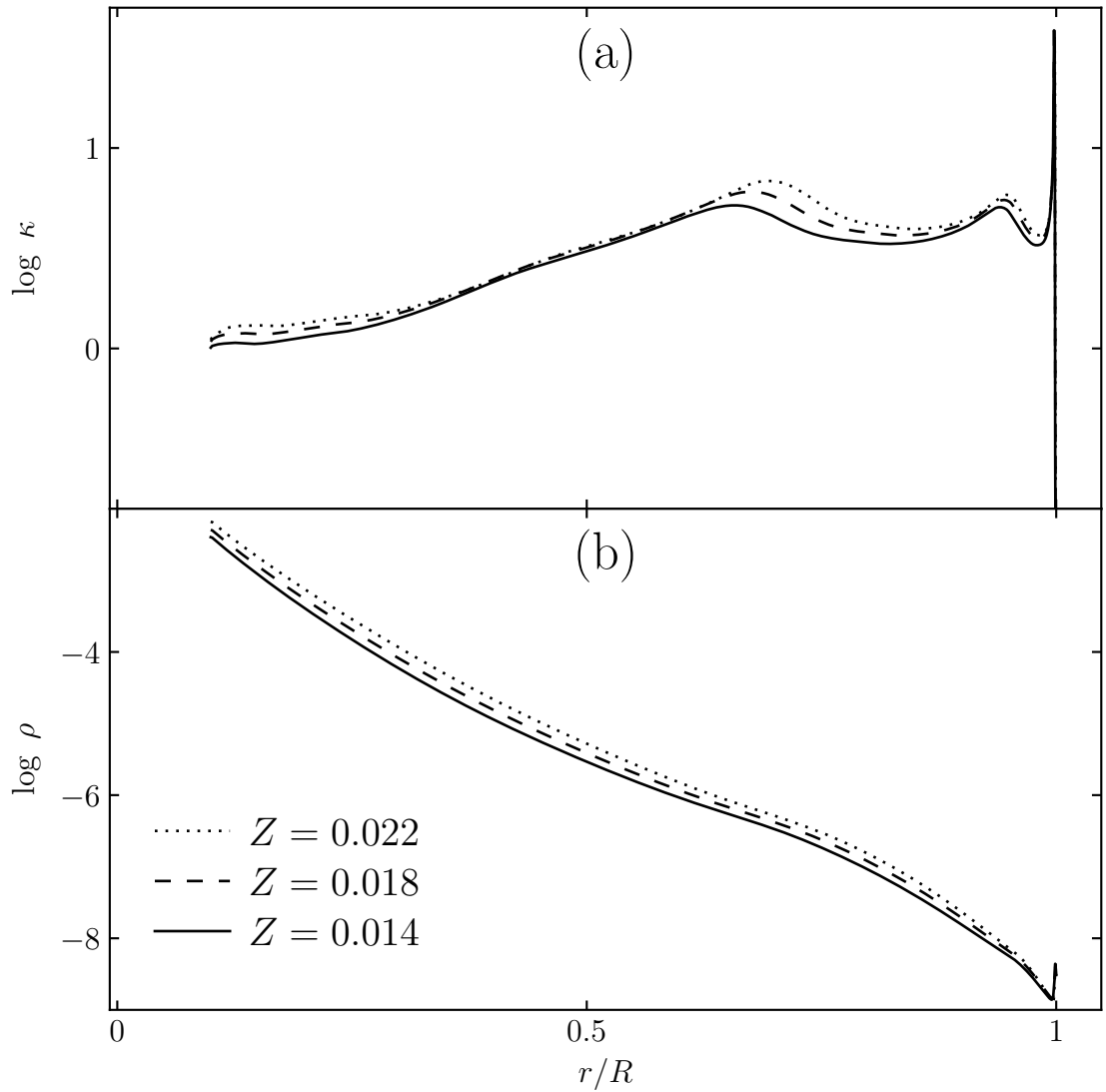


Fig. 2. The opacity coefficient κ (a) and the gas density ρ (b) as a function of radial distance from the stellar center r in hydrostatically equilibrium models at the oscillation mode swithing during the second crossing of the instability strip. Solid, dashed and dotted lines correspond to metal abundances $Z = 0.014$, 0.018 and 0.022 . R is the radius of the upper boundary of the evolutionary model.

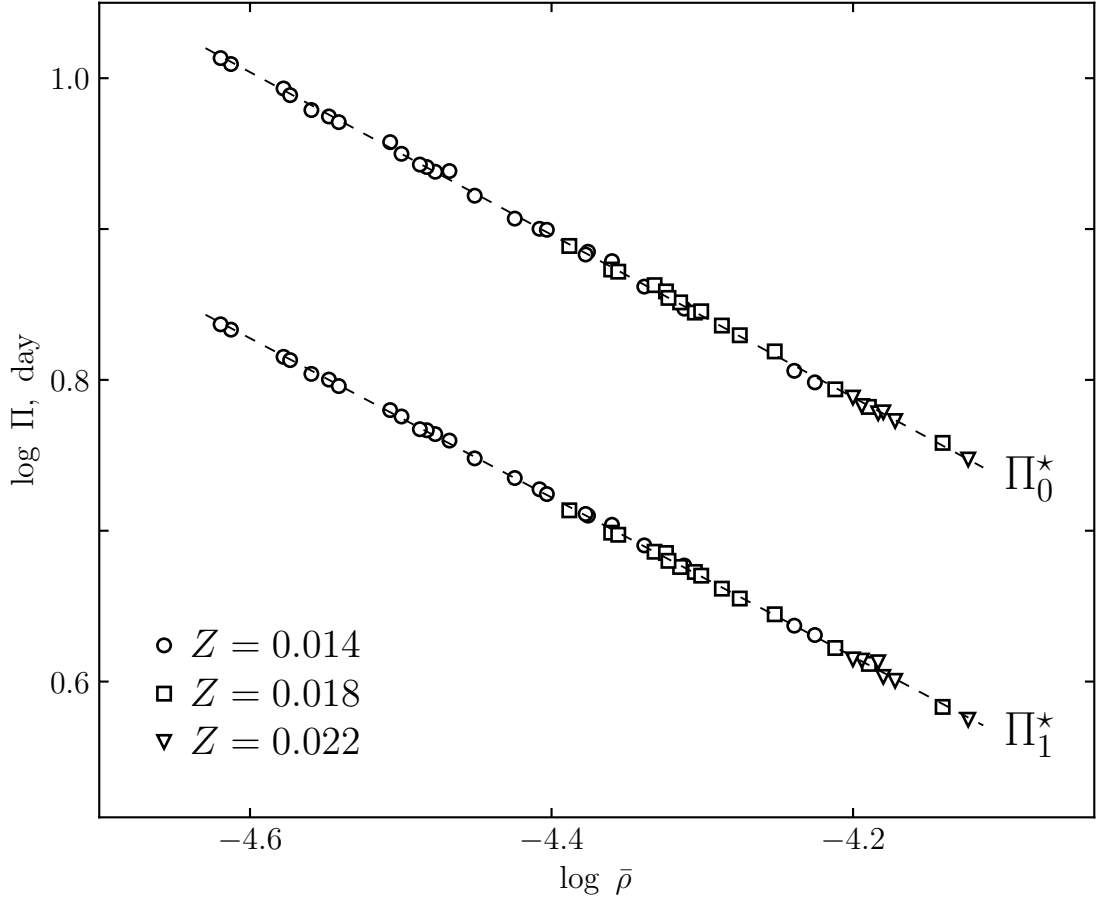


Fig. 3. Periods of the fundamental mode Π_0^* and the first overtone Π_1^* at the mode switching as a function of the mean density $\bar{\rho}$ for $Z = 0.014$ (open circles), $Z = 0.018$ (open squares) and $Z = 0.022$ (open triangles). Dashed lines show approximations by relations (1) and (2).

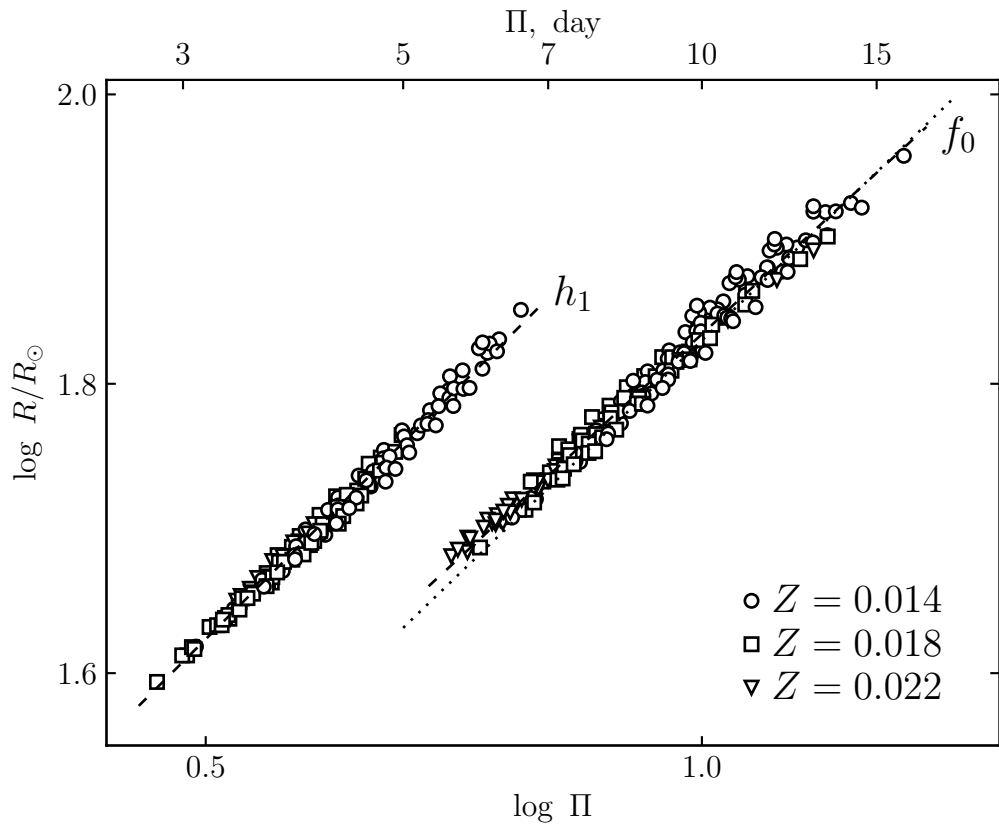


Fig. 4. Period–radius relations obtained from hydrodynamic computations for Cepheids pulsating in the fundamental mode (f_0) and in the first overtone (h_1). Dashed lines represent relations (3) and (4). Period–radius relation (5) from Lazovik and Rastorguev (2020) is shown by the dotted line.

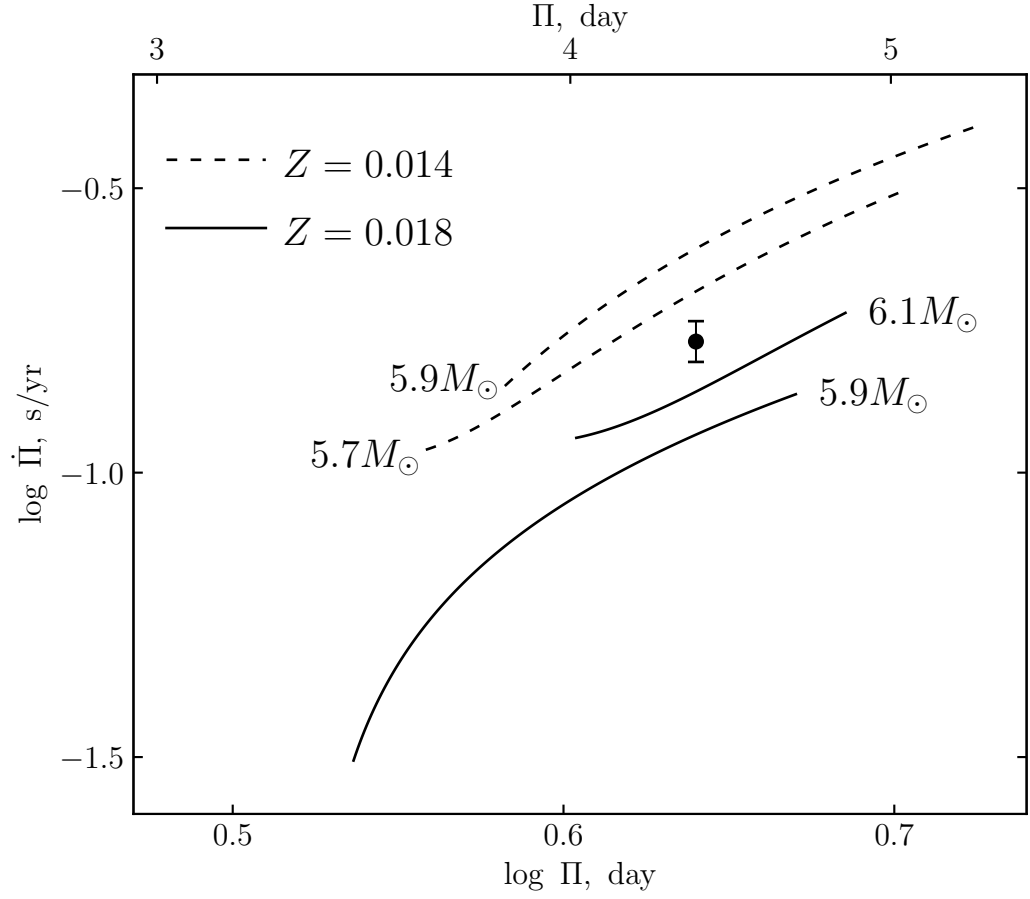


Fig. 5. The diagram $\Pi - \dot{\Pi}$ for Cepheid models pulsating in the first overtone during the third crossing of the instability strip for $Z = 0.014$ (dashed lines) and $Z = 0.018$ (solid lines). The initial mass M_0 is indicated at the curves. Observational estimates of Π и $\dot{\Pi}$ for CG Cas (Turner et al. 2008) are shown by the filled circle.